Available online at www.sciencedirect.com

SciVerse ScienceDirect

AASRI Procedia 1 (2012) 220 – 225

AASRI Procedia

www.elsevier.com/locate/procedia

2012 AASRI Conference on Computational Intelligence and Bioinformatics

Electric Field Induced by the Spin Current in a Semiconductor Dresselhaus Nanowire

Xi Fu[a,b,*], Feng Zhong[a]

[a]*Department of Electronic Engineering, Hunan University of Science and Engineering, Yongzhou 425100, China*
[b]*Key Laboratory of Low Dimensional Quantum Structures and Quantum Control (Hunan Normal University), Ministry of Education, Changsha 410081, China*

Abstract

Using a new spin current definition the spin current and spin-current-induced electric field in a weak semiconductor Dresselhaus spin-orbit coupling nanowire (quantum wire) have been investigated theoretically. It is found that two nonzero linear spin current density elements take on oscillation peaks at the center of nanowire and their strengths can be changed by the number of propagation modes and Dresselhaus constant, respectively. Moreover, the spin-current-induced electric field has been calculated and its strength is measurable with today's technology which can be used to spin current detection. Our consequences also show that the strengths of spin current and spin-current-induced electric field for the Dresselhaus case are smaller than that for the Rashba case.

Keywords: nanowire; spin current; electric field; Dresselhaus spin-orbit coupling.

1. Introduction

The intrinsic spin-orbit coupling (SOC) effect in semiconductors has attracted intensive attentions for its important role in semiconductor spintronics.[1, 2] There are two types of intrinsic SOC in semiconductor heterojunction two-dimensional electron gas (2DEG), namely Rashba SOC (RSOC) and Dresselhaus SOC (DSOC).[3, 4] In the situation of SOC, a moving spin is under an equivalent magnetic field with its strength depending on momentum of the particle. Similar to a system with an external magnetic field, it is natural to ask whether a persistent current exists in a SOC system.

doi:10.1016/j.aasri.2012.06.034

Spin current in the ballistic systems has been investigated in several years.[4-12] However, there still exists a lot of debates over the correct definition of spin current.[4, 6, 9, 10] Rashba first suggested that the conventional definition $\boldsymbol{I}_S = Re\,\Psi^{+}\hat{v}\hat{s}\Psi$ should be modified to eliminate the nonzero spin current.[4] After Rashba's work, Sun *et al*. bring forward a new definition by using the conventional (linear) spin current and a angular spin current describing the spin motion and rotation, and further they also discussed the reasonableness of this definition in details.[5, 7-11] In the following, we will use the definition studying spin current and spin-current-induced electric field in a weak Dresselhaus nanowire (quantum wire), and all nonzero spin current density elements are calculated and demonstrated analytically.

2. Model and formalism

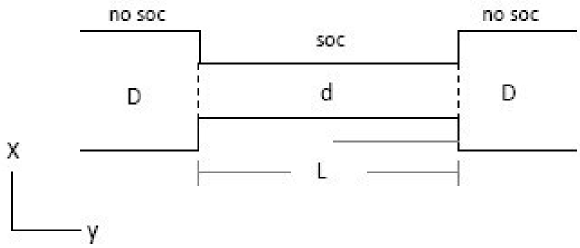

Fig. 1: The geometry of QW in which different width d is corresponding to different number of propagation modes.

The geometry model of quantum wire is shown in Fig.1 and its effective mass single electron Hamiltonian is [13]

$$H = -\frac{\hbar^2}{2m^*}\left(\frac{\partial^2}{\partial x^2} + \frac{\partial^2}{\partial y^2}\right) + V(x) + i\beta_D\left(\sigma_y\frac{\partial}{\partial y} - \sigma_x\frac{\partial}{\partial x}\right) \cdot \tag{1}$$

In the above Hamiltonian, the hard-wall confining potential is $V(x)$=0 for $|x|<d/2$ and ∞ for $|x|>d/2$ with d the width of QW. [9, 14] m^* and β_D denote effective electron mass and Dresselhaus constant respectively. The electron wave-function of Dresselhaus QW is two-components spinor $\Psi(x,y) = \begin{pmatrix}\psi_\uparrow(x,y)\\ \psi_\downarrow(x,y)\end{pmatrix}$ with the normalized wave-functions [15]

$$\psi_{\uparrow\downarrow}(x,y) = e^{ik_y y}\varphi_{\uparrow\downarrow}(x)/\sqrt{L_y} \tag{2}$$

in which the transverse eigenfunctions for the nth mode can be solved by perturbation method [16] as

$$\varphi_{\uparrow\downarrow}(x) = \varphi_n(x) = \sqrt{\frac{2}{d}}\sin\left[\frac{n\pi}{d}\left(x+\frac{d}{2}\right)\right] + i\sum_{m\neq n} C_{mn}\sin\left[\frac{m\pi}{d}\left(x+\frac{d}{2}\right)\right] \tag{3}$$

with

$$C_{mn} = \frac{4mn[1-(-1)^{m+n}]}{m^2-n^2}\frac{m^* d\beta_D}{\pi^2\hbar^2}(m,n=0,1,2,3,\ldots), \tag{4}$$

where L_y the length of QW. The electron energies are $E_{\uparrow\downarrow} = \hbar^2 k_{y\uparrow\downarrow}^2/2m^* + \varepsilon_{n\uparrow\downarrow}$ with the lateral sublevels $\varepsilon_{n\uparrow} = n^2\hbar^2\pi^2/(2m^* d^2) + \beta_D k_{y\uparrow}$ and $\varepsilon_{n\downarrow} = n^2\hbar^2\pi^2/(2m^* d^2) - \beta_D k_{y\downarrow}$, therefore, longitudinal wave-vectors for spin-up and -down electron can be expressed as

$$k_{y\uparrow}^{\pm}(E_\uparrow) = \frac{m^*}{\hbar^2}\left[-\beta_D \pm \sqrt{\beta_D^2 + 2\hbar^2(E_\uparrow - n^2\hbar^2\pi^2/(2m^* d^2))/m^*}\right], \tag{5}$$

$$k_{y\downarrow}^{\pm}(E_{\uparrow}) = \frac{m^*}{\hbar^2}[\beta_D \pm \sqrt{\beta_D^2 + 2\hbar^2(E_{\downarrow} - n^2\hbar^2\pi^2/(2m^*d^2))/m^*}]. \quad (6)$$

In order to calculate spin current density, we use the definition [9, 10]

$$j_{\omega}(r,t) = \mathrm{Re}\{\Psi^+(r,t)\hat{\omega}\times\hat{s}\Psi(r,t)\},\ j_s(r,t) = \mathrm{Re}\{\Psi^+(r,t)\hat{v}\hat{s}\Psi(r,t)\}, \quad (7)$$

where $\hat{v}$ and $\hat{\omega}$ are linear and angular velocity operator. The linear and angular spin-current-induced electric fields [9] $\vec{E}_s$ and $\vec{E}_{\omega}$ are

$$\vec{E}_s = \frac{\mu_0 g\mu_B}{\hbar}\int(\nabla'\cdot j_s)dV\times\frac{\vec{r}}{r^3},\ \vec{E}_{\omega} = -\frac{\mu_0 g\mu_B}{\hbar}\int\vec{j}_{\omega}dV\times\frac{\vec{r}}{r^3}, \quad (8)$$

Where $(\nabla'\cdot j_s)_i = \sum_j (d/dj)j_{s,ij}$ with i, j=x, y, z and μ_B the Bohr magneton. We use these symbols to represent spin current density elements, e.g. $j_{s,yx}$ represents linear spin current density element of an electron moving along the transverse y-direction with its spin in the longitudinal x-direction and $j_{\omega,x}$ represents electron spin precession in the x-direction.

After substituting the electron wave-function $\Psi(x,y)$ into Eq.(7), the linear and angular spin current density can be obtained straightforwardly. There are four nonzero linear spin current density elements

$$j_{s,yy} = \mathrm{Re}\{\frac{\beta_D}{2L_y}(\varphi_{\uparrow}^*\varphi_{\uparrow} + \varphi_{\downarrow}^*\varphi_{\downarrow})\},\ \ j_{s,yx} = \mathrm{Re}\{\frac{\hbar^2 k_y}{2m^*L_y}(\varphi_{\uparrow}^*\varphi_{\downarrow} + \varphi_{\downarrow}^*\varphi_{\uparrow})\} \quad (9)$$

$$j_{s,xx} = \mathrm{Re}\{-\frac{\beta_D}{2L_y}(\varphi_{\uparrow}^*\varphi_{\uparrow} + \varphi_{\downarrow}^*\varphi_{\downarrow}) - i\frac{\hbar^2}{2m^*L_y}(\varphi_{\uparrow}^*\varphi_{\downarrow}' + \varphi_{\downarrow}^*\varphi_{\uparrow}')\}, \quad (10)$$

$$j_{s,yz} = \mathrm{Re}\{i\frac{\beta_D}{2L_y}(\varphi_{\uparrow}^*\varphi_{\downarrow} + \varphi_{\downarrow}^*\varphi_{\uparrow})\}, \quad (11)$$

and one nonzero angular spin current density element

$$j_{\omega,z} = \mathrm{Re}\{\frac{\beta_D k_y}{L_y}(\varphi_{\uparrow}^*\varphi_{\downarrow} + \varphi_{\downarrow}^*\varphi_{\uparrow})\}. \quad (12)$$

From Eqs.(5) and (6) one can find four different occupied states for the nth mode, $k^+_{y\uparrow}$, $k^+_{y\downarrow}$, $k^-_{y\uparrow}$, $k^-_{y\downarrow}$, are in relation to the spin-up and spin-down states with electron propagating along $+y$ and $-y$ direction, respectively, and in the equilibrium these states have the relation $k^+_{y\uparrow} + k^+_{y\downarrow} + k^-_{y\uparrow} + k^-_{y\downarrow} = 0$ due to same contributions.[7, 10] Then the linear and angular spin current density elements for the nth mode which including k_y can be obtained as

$$j_{s,yx}^n = (j_{s,yx\uparrow}^{n+} + j_{s,yx\downarrow}^{n+} + j_{s,yx\uparrow}^{n-} + j_{s,yx\downarrow}^{n-})/4 = 0,\ j_{\omega,z}^n = (j_{\omega,z\uparrow}^{n+} + j_{\omega,z\downarrow}^{n+} + j_{\omega,z\uparrow}^{n-} + j_{\omega,z\downarrow}^{n-})/4 = 0, \quad (13)$$

and due to $\varphi_{\uparrow}^*\varphi_{\downarrow}$ and $\varphi_{\downarrow}^*\varphi_{\uparrow}$ are real

$$j_{s,yz} = \mathrm{Re}\{i\frac{\beta_D}{2L_y}(\varphi_{\uparrow}^*\varphi_{\downarrow} + \varphi_{\downarrow}^*\varphi_{\uparrow})\} = 0. \quad (14)$$

For the elements $j^n_{s,xx}$ and $j^n_{s,yy}$, their expression have not been changed because they are independent on k_y. Thus the total linear spin current density elements $j^T_{s,ij}$ can be calculated by summing $j^n_{s,ij}$ from the *1*th mode to the nth mode. [10] Furthermore, the linear spin-current-induced electric field $\vec{E}_s$ can be calculated as

$$\vec{E}_s = \frac{\mu_0 g\mu_B}{\hbar}\iint\frac{A_x[z\hat{e}_y - (y-y')\hat{e}_z]}{[(x-x')^2 + (y-y')^2 + (z-z')^2]^{3/2}}dx'dy', \quad (15)$$

where (x', y', z') and (x, y, z) the corresponding source and field position respectively, and $A_x = d\,j^T_{xx}(x')/dx'$.

The angular spin-current-induced electric field $\vec{E}_{\omega}=0$ and then the total spin-current-induced electric field $\vec{E}_T=\vec{E}_s+\vec{E}_{\omega}=E_{s,y}\hat{e}_y+E_{s,z}\hat{e}_z$.

3. Results and discussion

In the following, the numerical examples of nonzero linear spin current density elements and spin-current-induced electric field will be presented. The electron effective mass is taken as that for *InGaAs* quantum well $m^*=0.037m_e$ and the Dresselhaus constant $\beta_D=1.0\times10^{-12}$ eVm, moreover, the Bohr magneton $\mu_B=9.274\times10^{-24}$ A.m^2 and the factor g=2. In the situation of hard-wall potential confining, it is assumed that the QW is elongated with a fixed area $s=Ld$ and then the number of propagation modes (that is, the width of QW) will be decreased accordingly.[17] The initial length and width of QW are taken as L_0=300 nm and d_0=240 nm while the incident electron energies $E_{\uparrow\downarrow}=E_f$=5.9 *m*eV. For one mode to four modes case the width d is taken as 80 nm, 120 nm, 160 nm and 200 nm accordingly.

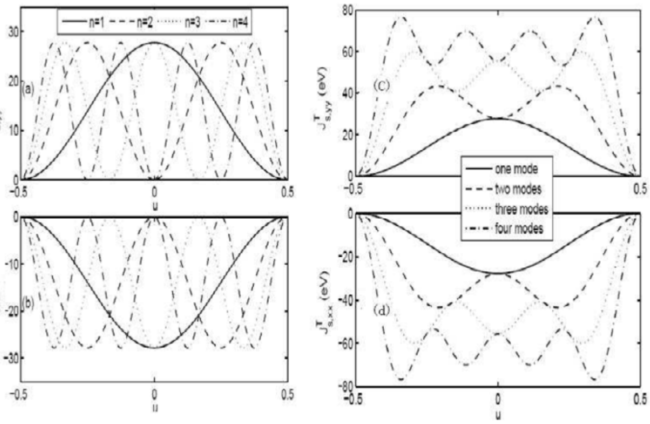

Fig. 2: The plots of $j^n_{s,xx}$ and $j^n_{s,yy}$, $j^T_{s,xx}$ and $j^T_{s,yy}$ as a function of no dimension coordinate $u=x/d$.

Figure 2 shows $j^n_{s,xx}$ and $j^n_{s,yy}$, $j^T_{s,xx}$ and $j^T_{s,yy}$ (summing $j^n_{s,xx}$ and $j^n_{s,yy}$ from the *1*th to the *n*th mode, respectively) as a function of no dimension coordinate $u=x/d$. From the figures one can find $j^n_{s,xx}$ and $j^n_{s,yy}$ show equal strengths and more oscillations for the *1*th to *4*th mode case, as well as when the number of propagation modes increasing, $j^T_{s,xx}$ and $j^T_{s,yy}$ also present more oscillations at the center of QW and their altitudes increase accordingly. It should be noted that $j^T_{s,xx}$ and $j^T_{s,yy}$ (or $j^n_{s,xx}$ and $j^n_{s,yy}$) do not have a inverse symmetry relation and the altitude of $j^T_{s,xx}$ (or $j^n_{s,xx}$) is a little larger than that of $j^T_{s,yy}$ (or $j^n_{s,yy}$) since two elements are different physical quantities. Furthermore, the nonzero element $j^T_{s,xx}$ (or $j^n_{s,xx}$) is special because it is the spin current density flowing along the confined x direction with the spin pointing to the transverse x direction. The existence of this element is due to spin precession in accompany with the electron motion.[7]

From Eq.(15) the direction of $\vec{E}_T$ ($\vec{E}_{\omega}$=0) can be known in the y-z plane and its strength can be expressed as $E_T=\sqrt{E^2_{s,y}+E^2_{s,z}}$. In Fig.3 (a)-(d), the contour patterns of E_T for one mode to four modes case are shown as functions of u and z. One can find that E_T mainly distributes at the nearby area of QW along the z direction and the area expands accordingly with the increasing of propagation modes. Furthermore, our results find that the spin-current-induced electric field for the Dresselhaus case is smaller than it for the Rashba case, moreover one can find when the number of propagation modes increases the strength of E_T decrease rapidly indicating that the DSOC has a less influence than the RSOC to the E_T.

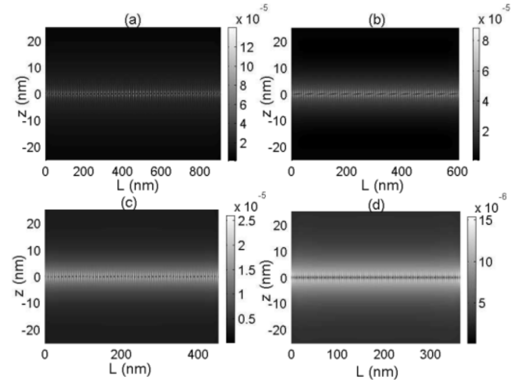

Fig. 3: The contour patterns of E_T for different modes case as functions of u and z.

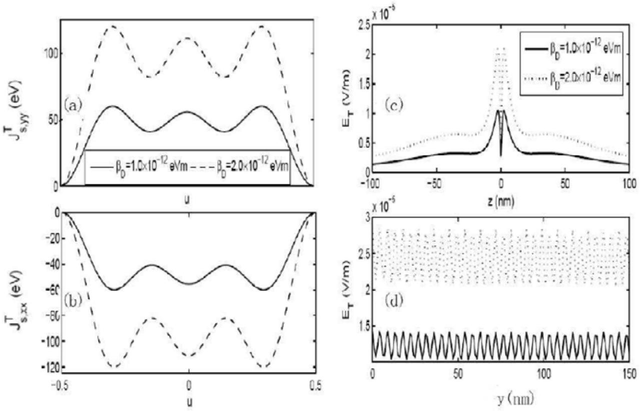

Fig. 4: The plots of $j^T_{s,xx}$, $j^T_{s,yy}$ and E_T for different Dresselhaus constant case with three modes in the QW.

In Fig.4 the influences of Dresselhaus constant β_D on $j^T_{s,xx}$, $j^T_{s,yy}$ and E_T for three modes case are demonstrated. It should be pointed out that in some 2DEG systems, the DSOC can lead to linear k-splitting and its strength increases with the decrease of thickness,[18] therefore, it would become comparable with the RSOC.[19] From the figures when β_D increases from 1.0×10^{-12} eVm to 2.0×10^{-12} eVm, the altitudes of $j^T_{s,xx}$, $j^T_{s,yy}$ and E_T increase for twice accordingly and a linear increasing relation with β_D exists. Furthermore, from Fig.4 (c) and (d) for the case of $\beta_D=2.0\times10^{-12}$ eVm (dashed line), E_T can reach ~10^{-5} V/m which is as much as that of mesoscopic semiconducting ring in Ref.10. Moreover, in Fig.4 (c) the electric potential difference between two points (60 nm, 200 nm, 2 nm) and (60 nm, 200 nm, 50 nm) for $\beta_D=2.0\times10^{-12}$ eVm can be calculated as about 0.289 nV which is also smaller than it for the RSOC case. However, this potential value is still measurable with today's technology [20] indicating that the spin-current-induced electric field can be detected which provide a way of spin current detection for the DSOC instance.

4. Conclusion

In this paper, we have studied the spin current and spin-current-induced electric field in a Dresselhaus nanowire (quantum wire). Using the electron wave-functions and definition of spin current, the linear and angular spin current densities and its induced electric fields have been calculated. It is found that two nonzero linear spin current density elements have peaks at the center of nanowire and their strengths can be changed by the number of propagation modes and Dresselhaus constant. Moreover, for the Dresselhaus QW instance the spin-current-induced electric field can also be detected which makes a way of spin current detection.

Acknowledgements

Project supported by the Open Project of Key Laboratory of Low Dimensional Quantum Structures and Quantum Control (Hunan Normal University), Ministry of Education of China under Grant No QSQC1002.

References

[1] Wolf S A, Awschalom D D, Buhrman R A, Daughton J M, Moln´ar S V, Roukes M L, Chtchelkanova A Y, Treger D M. Spintronic: A spin-based electronics vision for the future. Science 2001; 294: 1488-1495.

[2] Datta S, Das B. Electronic analog of the electro-optic modulator. Appl. Phys. Lett. 1989; 56: 665-667.

[3] Hu C M, Nitta J, Akazaki T, Takayanagai H, Osaka J, Pfeffer P, Zawadzki W. Zero-field spin splitting in an inverted $In_{0.53}Ga_{0.47}As/In_{0.52}Al_{0.48}$ As heterostructure: Band nonparabolicity influence and the subband dependence. Phys. Rev. B 1999; 60: 7736-7739; Grundler D. Large Rashba splitting in InAs quantum wells due to electron wave function penetration into the barrier layers. Phys. Rev. Lett. 2000; 84: 6074-6077.

[4] Rashba E I. Spin currents in thermodynamic equilibrium: The challenge of discerning transport currents. Phys. Rev. B 2003; 68: 241315(R).

[5] Ambegaokar V, Eckern U. Coherence and persistent currents in mesoscopic rings. Phys. Rev. Lett. 1990; 65: 381-384.

[6] Splettstoesser J, Governale M, Z¨ulicke U. Persistent current in ballistic mesoscopic rings with Rashba spin-orbit coupling. Phys. Rev. B 2003; 68: 165341; Lee M, Choi M S. Ballistic spin currents in mesoscopic metal/In(Ga)As/metal junctions. Phys. Rev. B 2005; 71: 153306.

[7] Sun Q F, Xie X C. Persistent spin current in spin-orbit coupling systems in the absence of an external magnetic field. Int. J. Mod. Phys. B 2007; 21: 3687-3690.

[8] Sun Q F, Guo H, Wang J. Spin-current-induced electric field. Phys. Rev. B 2004; 69: 054409; Sun Q F, Xie X C, Wang J. Persistent spin current in a mesoscopic hybrid ring with spin-orbit coupling. Phys. Rev. Lett. 2007; 98: 196801.

[9] Sun Q F, Xie X C. Definition of the spin current: The angular spin current and its physical consequences. Phys. Rev. B 2005; 72: 245305.

[10] Sun Q F, Xie X C, Wang J. Persistent spin current in nanodevices and definition of the spin current. Phys. Rev. B 2008; 77: 035327.

[11] Wang Y, Zhou G H. Persistent spin current in a quantum wire with weak Rashba spin-orbit coupling. Chin. Phys. Lett. 2006; 23: 3065.

[12] Zhou X, Zhang Z Y, Hu C Z. Spin continuity equation and definition of spin current. arXiv 2009: 0904.3796v2.

[13] Chang M C. Effect of in-plane magnetic field on the spin Hall effect in a Rashba-Dresselhaus system. Phys. Rev. B 2005; 71: 085315; Yang W, Chang K. Magnetotransport in two-dimensional electron gas: The interplay between spin-orbit interaction and Zeeman splitting. Phys. Rev. B 2006; 73: 045303.

[14] Shi J R, Zhang P, Xiao D, Niu Q. Proper Definition of Spin Current in Spin-Orbit Coupled Systems. Phys. Rev. Lett. 2006; 96: 076604.

[15] Wang X F, Vasilopoulos P. Band structure and magnetotransport of a two-dimensional electron gas in the presence of spin-orbit interaction. Phys. Rev. B 2005; 72: 085344.

[16] Moroz A V, Barnes C H W. Effect of the spin-orbit interaction on the band structure and conductance of quasi-one-dimensional systems. Phys. Rev. B 1999; 60: 14272-24285.

[17] Kassubek F, Stafford C A, Grabert H. Force, charge, and conductance of an ideal metallic nanowire. Phys. Rev. B 1999; 59: 7560-7574.

[18] D'yakonov M I, Kachorovskii V Yu. Spin relaxation in n-modulation doped GaAs-AlGaAs (110) quantum wells. Sov. Phys. Semicond. 1986; 20: 110-113.

[19] Lommer G, Malcher F, R¨osler U. Spin splitting in semiconductor heterostructure for $B \rightarrow 0$. Phys. Rev. Lett. 1988; 60: 728-731.

[20] Sch¨utz F, Kollar M, Kopietz P. Persistent spin currents in mesoscopic Haldane-gap spin rings. Phys. Rev. B 2004; 69: 035313; Bruno P, Dugaev V K. Equilibrium spin currents and the magnetoelectric effect in magnetic nanostructures. Phys. Rev. B 2005; 72: 241302(R) .